Characterization of Cardiac Quiescence from Retrospective Cardiac Computed Tomography Using a Correlation-Based Phase-to-Phase Deviation Measure

Carson A. Wick* and James H. McClellan†
School of Electrical and Computer Engineering, Georgia Institute of Technology, 777 Atlantic Drive NW, Atlanta, GA 30332, USA

Chesnal D. Arepalli‡
Division of Cardiothoracic Imaging, Department of Radiology and Imaging Sciences, Suite 309, 1364 Clifton Road NE, Atlanta, GA 30322, USA

Adam M. Coy§
School of Medicine, Emory University, 100 Woodruff Circle, Atlanta, GA 30322, USA

Srini Tridandapani¶
Department of Radiology and Imaging Sciences, Emory University, Winship Cancer Institute, 1701 Uppergate Drive NE, Suite 5018, Atlanta, GA 30322, USA

(Dated: February 12, 2014)

Objective: Accurate knowledge of cardiac quiescence is crucial to the performance of many cardiac imaging modalities, including computed tomography coronary angiography (CTCA). To accurately quantify quiescence, two novel methods for detecting the quiescent periods of the heart from retrospective cardiac computed tomography (CT) using a correlation-based, phase-to-phase deviation measure were developed. **Methods:** Two novel methods were developed to investigate quiescence of individual coronary vessels as well as the interventricular septum (IVS). Retrospective cardiac CT data were obtained from 20 patients (11 male, 9 female, 33-74 years) and the left-main, left-anterior-descending, left-circumflex, and right-coronary arteries were segmented for each phase. As an easily identifiable feature, the interventricular septum (IVS) was analyzed to assess how well it predicts vessel quiescence. **Results:** The motion of the vessels was found to be similar to each other but less so as heart rate increases. Similarly, the IVS was found to be a reliable predictor of vessel quiescence, but less so at higher heart rates. **Clinical Impact:** The methods and results presented in this work will be used to develop new CTCA gating techniques and quantify the resulting potential improvement in CTCA image quality.

I. INTRODUCTION

Cardiac quiescence during data acquisition is imperative to obtain diagnostic images of the coronary vessels for imaging modalities requiring extended data acquisition times, such as computed tomography (CT) and magnetic resonance imaging (MRI) [1]. To minimize motion artifacts and blurring in cardiac images, it is necessary to acquire imaging data when the heart is relatively stationary, i.e., during quiescent periods of the cardiac cycle. Current methods for triggering acquisition rely almost exclusively on the electrocardiogram (ECG). However, the ECG serves only as a proxy for the mechanical state of the heart and has been shown to be imprecise in predicting quiescent phases due to subject and heart-rate variability [2, 3]. Therefore, it is desirable to detect and predict quiescence from a signal that is more indicative of cardiac motion. For this work, quiescent periods of the coronary vessels and interventricular septum (IVS) will be detected from retrospective cardiac CT data using two methods based on a robust correlation-based, phase-to-phase deviation measure. The results of this work will inform the development of more accurate methods for predicting cardiac quiescence based on signals derived directly from the mechanics of the heart.

The imaging performance of both cardiac CT and MRI relies heavily on trigged data acquisition during quiescent periods of the cardiac cycle, i.e., cardiac gating. Accurate gating is necessary to minimize motion artifacts and ensure that the heart is in the same position in the imaging plane for techniques requiring data acquisition over multiple cardiac cycles. One application where accurate gating is crucial is CT coronary angiography (CTCA) [1].

CTCA is a promising alternative to the much more invasive catheter coronary angiography (CCA). More than 1.1 million CCAs are performed annually in the United States of America costing approximately $40 billion and resulting in more than 14,000 major complications [4].

* carson@gatech.edu
† jim.mcclellan@gatech.edu; Supported by the John and Marilu McCarty Chair.
‡ chesnaldey@gmail.com
§ adam.coy@emory.edu
¶ stridan@emory.edu; Supported by the PHS Grant (KL2 RF025009) from the Clinical and Translational Science Award program, National Institutes of Health, National Center for Research Resources, and in part by Award Number K23EB013221 from the National Institute of Biomedical Imaging and Bioengineering.

Furthermore, nearly 40% of these tests reveal no coronary artery disease (as defined by less than 20% vessel stenosis) [5]. Conversely, CTCA does not require catheterization and is thus a less invasive and more cost-effective alternative.

For this work cardiac quiescence is estimated from retrospective cardiac CT studies. Reconstructions were obtained at one percent increments from 20% to 80% of the cardiac cycle for 20 subjects. Cardiac phase (%) is defined using the R-R interval of the ECG. For each reconstruction, five cardiac features are segmented using a manually-guided, semi-automated approach. The features include the IVS and the left main (LM), left anterior descending (LAD), left circumflex (LCX), and right coronary (RCA) arteries. The IVS is segmented to compare IVS motion to that of the coronary vessels. Using a robust deviation measure based on the phase-to-phase correlation of each of these five cardiac features, the quiescence characteristics of the coronary vessels were investigated.

The remainder of this paper is organized as follows. The methods for data acquisition, cardiac feature segmentation, and quiescence analysis are presented in Section II. In Section III, the results of the quiescence characterization of each observed cardiac feature for the 20 subjects are provided. Lastly, a discussion on the application of the methods and the implications of this work on cardiac imaging is given in Section IV.

II. METHODS AND PROCEDURES

A. Data Acquisition

Retrospective cardiac CT data were acquired from 20 human subjects (11 male, 9 female, 33-74 years) using a Siemens Somatom Definition dual-source 64-slice CT scanner (Siemens, Erlangen, Germany). These subjects were examined independently of this study for various cardiac conditions and the data were collected retroactively with the approval of the Emory University Institutional Review Board. CT volume reconstructions were created at one percent increments of the cardiac cycle from 20% to 80% based on the electrocardiogram (ECG) signal used for gating during data acquisition.

B. Segmentation of Cardiac Features

Segmentation of the coronary vessel and IVS features is performed using a manually-guided, semi-automated approach wherein the feature is manually segmented for an undersampled number of axial slices containing the feature, i.e., each manually-segmented slice is separated by one or more non-manually-segmented slices. The manual segmentations were performed by a graduate researcher under the guidance of a radiologist. The segmentations of the feature for the remaining slices are calculated using an interpolation scheme based on the signed distance function (SDF) of the two neighboring, manually-segmented slices. The final three-dimensional (3D) segmentation is then constructed by combining all of the segmented slices.

The set of pixels defining the location of the feature in a given slice form a set S. The SDF of S is defined as

$$\phi_S(x,y) = \begin{cases} d_S(x,y) & \text{if } (x,y) \in S \\ -d_S(x,y) & \text{if } (x,y) \notin S \end{cases} \tag{1}$$

where $d_S(x,y)$ is the Euclidean distance from the point (x,y) to the nearest point on the boundary of S. It follows that $\phi_S(x,y)$ will be zero on the boundary of S and greater than zero inside S.

The segmentations of the non-manually-segmented slices are interpolated from the SDF of the two nearest-neighboring, manually-segmented slices. Note that the manually-segmented slices may have more than one slice between them. Let $\phi_{S_z}(x,y)$ be the SDF for the axial slice at height z. The slice interpolation scheme is then defined as

$$\phi_{S_z}(x,y) = \frac{(z^+ - z)\phi_{S_{z^-}} + (z - z^-)\phi_{S_{z^+}}}{z^+ - z^-},\ z^- < z < z^+ \tag{2}$$

where z^- and z^+ are the heights of the nearest lower and higher manually segmented slices, respectively. The segmentation for each slice at a height z is then defined as the set of points, (x,y), where $\phi_{S_z}(x,y)$ is greater than or equal to zero, i.e.,

$$\{S_z \in \mathbb{R}^2 : S_z = (x,y),\ \phi_{S_z}(x,y) \geq 0\}. \tag{3}$$

The final 3D segmentation, V, is obtained by combining all of the segmented slices, i.e.,

$$\{V \in \mathbb{R}^3 : V = (x,y,z),\ z_{min} \leq z \leq z_{max},\ (x,y) \in S_z\} \tag{4}$$

where z_{min} and z_{max} are the lower and upper boundaries of the cardiac feature in the axial direction.

C. Identification of Intra-Feature Cardiac Quiescenct Periods

Quiescent periods of the coronary vessels and the IVS are calculated using a correlation-based, phase-to-phase deviation measure. In short, the deviation between a segmented feature at a given cardiac phase and neighboring phases is computed. This deviation measure will decrease as the cardiac feature becomes more quiescent.

For this work, the deviation between cardiac phases is expressed as a negative function of the Pearson correlation coefficient taken over the feature volume. This method is a 3D analogue to the method proposed by the authors to analyze cardiac quiescence from echocardiography in [6]. The Pearson correlation coefficient has been

shown to be a strong indicator of image similarity and as such can be interpreted as a measure of the similarity of the feature position between two phases [7]. The correlation coefficent between two phases, i and j, is given as

$$\rho_{V_s}(i,j) = \frac{\sum_{(x,y,z)\in V_s}(I_i(x,y,z)-\bar{I}_i^{V_s})(I_j(x,y,z)-\bar{I}_j^{V_s})}{\sqrt{\sum_{(x,y,z)\in V_s}(I_i(x,y,z)-\bar{I}_i^{V_s})^2 \sum_{(x,y,z)\in V_s}(I_j(x,y,z)-\bar{I}_j^{V_s})^2}} \quad (5)$$

where I_i is the imaged volume at phase i, V_s is a static set of voxels containing the feature for all phases, and $\bar{I}_i^{V_s}$ is the mean of I_i in V_s.

Here V_s is chosen to be the union of the segmentations for all phases and is defined as

$$V_s = \bigcup_i V_i \quad (6)$$

where V_i is the set of voxels in $\mathbb{R}^3$ indicating the segmentation for cardiac phase i. This choice of V_s provides the smallest set containing the segmentations of all phases.

The phase-to-phase deviation is calculated as

$$\mathbf{D}(i,j) = 1 - \rho_{V_s}(i,j) \quad (7)$$

for all possible phase-to-phase pairs. The resulting *deviation matrix* for a specific vessel can then be viewed as an image allowing for the quiescent phases to be readily identified visually. An example of $\mathbf{D}(i,j)$ for the LM, LAD, LCX, and RCA of Subject 2 viewed as images is shown in Fig. 1 with blue regions along the diagonal corresponding to quiescent phases.

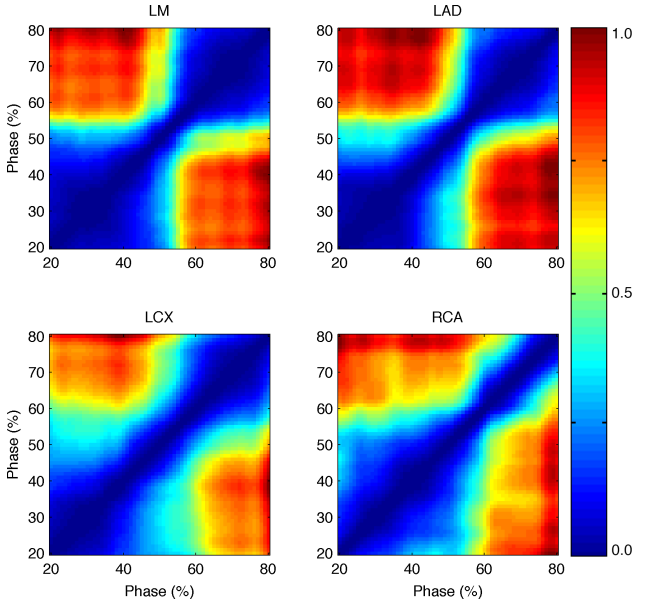

FIG. 1. Deviation matrices for the LAD, LM, LCX, and RCA of Subject 2. Blue regions along the diagonal correspond to quiescent phases. The one-off diagonal, $\mathbf{D}(i,i-1)$, is indicated by a white line on the deviation matrix of the LM. Note that the diagonal runs from the lower left to upper right of each matrix.

1. *Aggregate Vessel Deviation*

To investigate the motion of the coronary vessels taken in aggregate for each subject, a deviation matrix is formed from the union of the four static volumes representing the LAD, LM, LCX, and RCA found using Eq. 6. That is, the aggregate deviation for all vessels for each subject is defined as

$$\mathbf{D}_{agg}(i,j) = 1 - \rho_{V_{agg}}(i,j) \quad (8)$$

where V_{agg} is the union of all vessel segmentations for a given subject.

2. *Quiescence from Approximated Velocity*

The magnitude of the velocity of the vessel in the direction orthogonal to the primary axis of the vessel is approximately proportional to the phase-to-phase deviation. This holds because the value of $\mathbf{D}(i,j)$ is approximately linear with vessel displacement in the orthogonal direction. This approximation holds as long as between phases i and j the vessel is cylindrical, does not deform, moves linearly, and is displaced less than the feature radius. Because the phase delay between neighboring cycles is only one percent, the velocity magnitude can be approximated by the deviation between sequential phases defined as

$$v_{app}(i) = \mathbf{D}(i,i-1) \quad (9)$$

where $v_{app}(i)$ is the approximated velocity of the vessel at phase i, and $\mathbf{D}(i,i-1)$ is the one-off diagonal of the deviation matrix.

For this work, quiescent periods are defined from the velocity approximation as phases of the cardiac cycle when $v_{app}(i)$ is less than the mean of $v_{app}(i)$. This choice was made to ensure that each vessel was thresholded in a comparable manner. An example of this process for the LM of Subject 2 is provided in Fig. 2.

3. *Identification of Optimal Quiescent Phases*

Ideally, the acquisition time of the CT scanner should be taken into account in identifying quiescent phases. This is accomplished by finding the minimum of an averager operating on a square neighborhood sliding along the diagonal of $\mathbf{D}(i,j)$. The mean of the square neighborhood corresponds to the similarity of the consecutive phases that make up the neighborhood. The size of the square neighborhood is chosen to correspond to the data

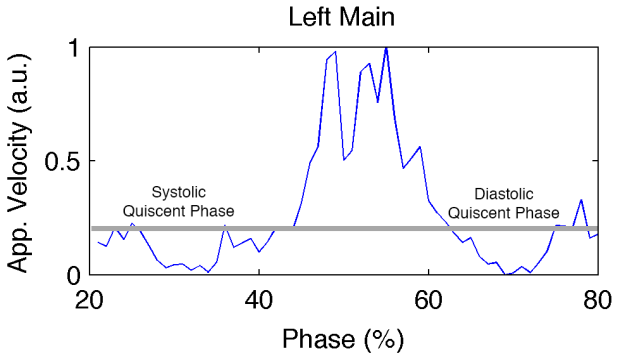

FIG. 2. Normalized approximated velocity of the LM for Subject 2 with the systolic and diastolic quiescent periods indicated. The threshold for quiescence is chosen to be the mean of the approximated velocity signal, indicated in the figure by the grey line.

acquisition time of the CT scanner. For this work the acquisition time is 83 ms, corresponding to the quarter gantry rotation time taken by a dual-source CT scanner with a rotation time of 333 ms. As an example, for a subject with a heart rate of 60 bpm, one percent of the cardiac cycle will equal 10 ms. Therefore, a neighborhood covering eight percent will approximately cover the 83 ms necessary for data acquisition. By finding the neighborhood with the minimum mean deviation, the optimal quiescent phase is found. The output of the moving averager, called the *deviation signal*, can be expressed as

$$d(i) = \frac{1}{N^2} \sum_{n_1=-N/2}^{N/2} \sum_{n_2=-N/2}^{N/2} \mathbf{D}(i+n_1, i+n_2), \qquad (10)$$

where N is the width of the neighborhood. A graphical representation of this idea is provided by Fig. 3 where the moving averager operating on $\mathbf{D}(i,j)$ and the resulting $d(i)$ are shown for the LM of Subject 2. Note that the deviation signal is a smoothed version of the approximated velocity shown in Fig. 2.

D. Comparison of Inter-Feature Cardiac Quiescence

The similarity of the deviation signals from Section II C 3 is found using a weighted correlation technique to compare the $d(i)$ for pairs of features. The correlation used is a modification of the the standard Pearson correlation measure that is weighted more heavily in regions where $d(i)$ is smaller, e.g., more quiescent. The weighted correlation is defined as

$$\rho_w(d_x, d_y) = \frac{\sum_n w(n)(d_x(n) - \bar{d}_x)(d_y(n) - \bar{d}_y)}{\sqrt{\sum_n w(n)(d_x(n) - \bar{d}_x)^2 \sum_n w(n)(d_y(n) - \bar{d}_y)^2}} \qquad (11)$$

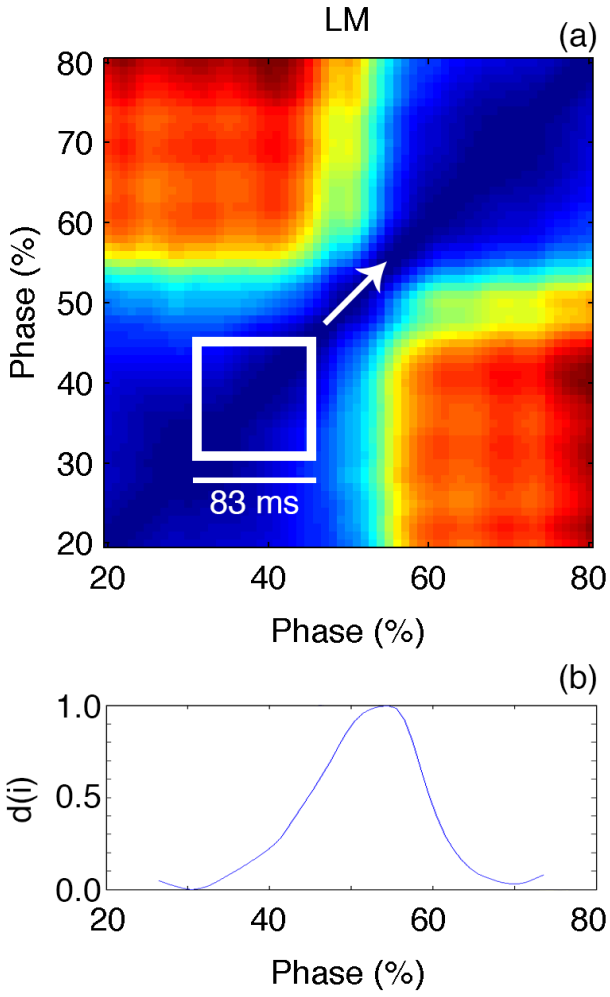

FIG. 3. Deviation matrix (a) for the LM of Subject 2 showing the moving averager operating on a square neighborhood with a size corresponing to 83 ms. Note that the diagonal runs from the lower left to upper right of the deviation matrix. The normalized output of the moving averager, $d(i)$, is shown in (b).

where d_x and d_y are the deviation signals of the two features, w is the weighting vector, and $\bar{d}$ is the weighted mean of d. For this work the weight vector is defined as the normalized distance from the maximum to the minimum of the average of d_x and d_y. This can be expressed as

$$w(i) = \frac{\hat{d}_{max} - \hat{d}(i)}{\hat{d}_{max} - \hat{d}_{min}} \qquad (12)$$

where $\hat{d}(i) = (d_x(i) + d_y(i))/2$, and $\hat{d}_{min}$ and $\hat{d}_{max}$ are the minimum and maximum of $\hat{d}(i)$, respectively. This choice of weighting vector results in $w = 0$ for $\hat{d}(i) = \hat{d}_{max}$ and $w = 1$ for $\hat{d}(i) = \hat{d}_{min}$. An example of the deviation signals for the IVS and the aggregate vessel motion are given in Fig. 4. The two signals are normalized to have zero

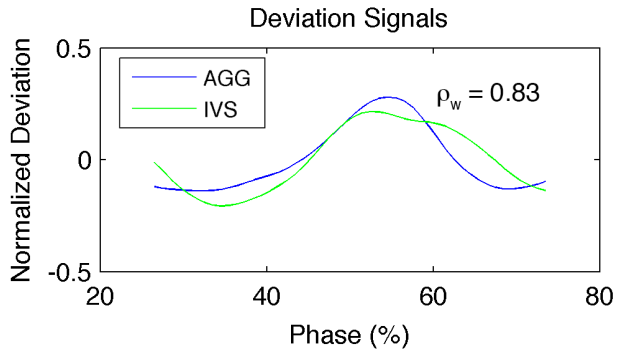

FIG. 4. Deviation signals for the IVS and aggregate vessel motion, normalized to have zero mean and unit power. The two signals have a weighted correlation of 0.8301 calculated from Eq. 11.

mean and unit power, and have a weighted correlation of 0.8301.

III. RESULTS

The reconstructed CT volumes for each of the 20 subjects were segmented and the motion of the LM, LAD, LCX, RCA, and IVS was investigated. The approximated velocity magnitude of each of the cardiac features was found and used to identify the center and duration of the quiescent periods of each feature. The optimal quiescent phase for each feature was found using the method described in Section II C 3. Subsequently, by using the deviation signal comparison technique described in Section II D, the IVS was found to be a suitable predictor of aggregate vessel quiescence.

A. Segmentation of the Coronary Vessels and Interventricular Septum

The LM, LAD, LCX, RCA, and IVS were segmented using the approach outlined in II B. The average ratio of total number of segmented slices to the number of manually-segmented slices was three and eight for the coronary vessels and IVS, respectively. These ratios indicate the overall segmentation speed-up achieved by using the proposed method, rather than manually segmenting each slice.

B. Identification of Quiescent Periods for the Coronary Vessels and the Interventricular Septum

1. *Center and Duration of Quiescent Periods*

The center and duration of the systolic and diastolic quiescent periods of the LM, LAD, LCX, RCA, and IVS were calculated using the method described in II C 2. The systolic quiescent period was defined as the longest quiescent phase with a center occurring before 60% of the cardiac cycle as defined by the R-R interval of the ECG. The diastolic quiescent period was defined in the same manner but with a center occurring at or later than 60%. The results of these calculations are shown in Fig. 5 where the systolic and diastolic quiescent periods for each subject are plotted against the heart rate of the subject.

TABLE I. Quiescent Period Statistics (%)

HR	Feature	Systolic Periods		Diastolic Periods	
		Center	Duration	Center	Duration
Low					
	LM	32.1±4.2	15.1±4.7	69.8±2.5	21.2±5.2
	LAD	31.0±2.0	18.3±5.2	69.0±3.2	19.7±7.6
	LCX	33.9±5.5	17.2±6.2	69.8±4.0	21.0±8.0
	RCA	35.5±4.8	14.7±4.5	70.9±1.0	19.2±2.0
	IVS	31.9±1.6	13.8±3.8	70.3±1.3	20.5±2.6
Med.					
	LM	38.5±3.4	22.0±4.5	71.6±2.2	17.8±4.4
	LAD	33.8±3.5	16.7±7.5	71.5±2.6	18.0±5.2
	LCX	38.6±2.4	16.7±4.7	70.5±1.4	19.3±2.6
	RCA	37.3±4.0	17.7±5.8	72.9±1.1	14.5±3.3
	IVS	35.8±5.4	16.2±3.3	71.8±1.5	17.5±3.0
High					
	LM	38.1±4.1	24.0±5.8	68.0±4.3	7.8±5.7
	LAD	36.9±6.3	24.4±6.8	69.8±4.2	6.6±4.2
	LCX	37.1±6.8	23.5±8.7	70.7±5.7	7.4±6.4
	RCA	37.4±4.9	26.4±6.3	70.2±5.6	7.0±5.7
	IVS	35.8±6.1	20.0±7.6	74.0±4.0	9.5±8.7

From Fig. 5, the position and duration of the quiescent phases exhibit a large amount of inter-subject variability. This suggests that the ECG alone may be suboptimal in terms of predictive accuracy of cardiac quiescence.

The subjects were separated into low (below 65 bpm), medium (from 65 to 85 bpm), and high (above 85 bpm) heart rate ranges. There were 6 subjects with low heart rates, 6 with medium heart rates, and 8 with high heart rates. The tabulated results of each vessel for each range are provided in Table I.

From Fig. 5 and Table I, the duration of the systolic phases in terms of percent of the cardiac cycle can be seen to increase with heart rate, while that of the diastolic phases can be seen to decrease with heart rate. This agrees with the accepted standard that at higher heart rates cardiac imaging data should be obtained during systole [1].

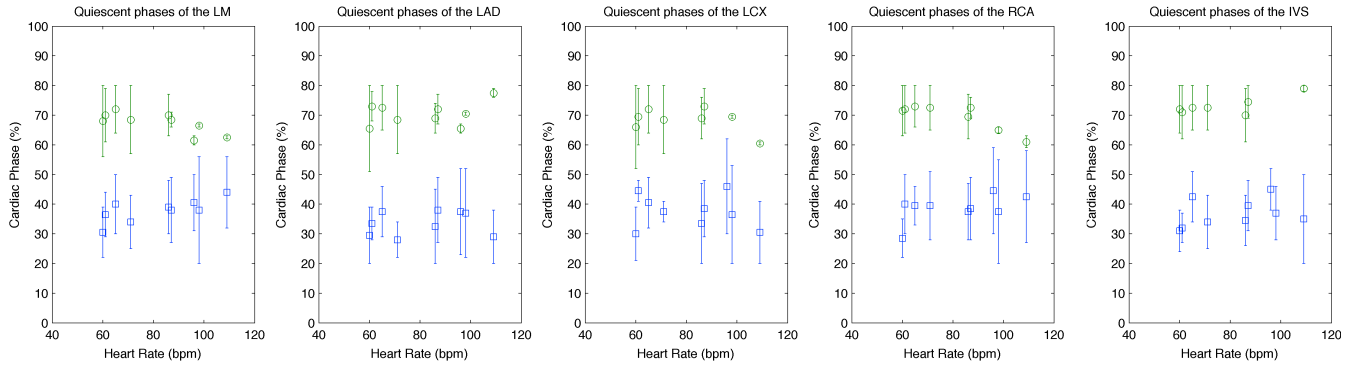

FIG. 5. Quiescent periods of the LM, LAD, LCX, RCA, and IVS. Systolic quiescent phases are blue and diastolic quiescent phases are green. The centers of the quiescent periods are indicated by the marker and the durations by the length of the lines extending from the period centers.

TABLE II. Optimal Quiescent Phase Statistics (%)

Feature	Low HR	Medium HR	High HR
LM	74.1± 1.9	62.4±16.6	38.6± 5.7
LAD	72.8± 3.0	66.8±16.0	37.2± 7.5
LCX	67.6±14.7	66.8±15.0	39.2±10.5
RCA	67.4±13.6	45.9±14.5	39.9± 6.3
AGG	67.6±17.5	67.6±14.7	39.2± 3.2
IVS	74.9± 2.0	74.8± 1.6	52.3±17.8

2. *Optimal Quiescent Phases*

The optimal quiescent phase of each cardiac feature was found for all 20 subjects. This was accomplished by determining the minimum of the deviation signal $d(i)$ as defined in Eq. 10. In addition, the optimal quiescent phase of the vessels taken in aggregate was computed from the aggregate deviation matrix as defined in Eq. 8. The subjects were separated into low, medium, and high heart rate ranges, as before. A summary of the statistics is provided in Table II. Note that a high standard deviation for a given heart rate range corresponds to some optimal phases being in systole and some in diastole. This is most apparent for medium heart rates (from 65 to 85 bpm) because the optimal phase transitions from diastole to systole in this heart rate range.

An interesting conclusion that can be drawn from Table II is that the optimal quiescent phase of the RCA transitions to systole at a lower heart rate than the other vessels and that the optimal phase of the IVS transitions to systole at a higher heart rate than the coronary vessels. Also of note is that the optimal quiescent phase of the vessels when taken in aggregate is very similar to each individual vessel with the exception of the RCA.

C. Inter-Feature Comparison of Deviation Signals

The deviation signals for each cardiac feature were compared for all subjects using the weighted correlation technique described in Section II D. In addition to comparing each feature to every other feature, the IVS was compared to the aggregate deviation signal representing all vessels. This comparison was performed in order to observe the similarity of the deviation signal of the IVS to the coronary vessels taken as a whole. Prior to calculating the weighted correlation, all signals were normalized to have zero mean and unit power. The summary of the comparison is presented in Table III with the subjects separated into low, medium, and high heart rate ranges as described in Section III B 1. An example of two deviation signals with a weighted correlation of 0.83 is provided in Fig. 4.

The similarity of the deviation signals tends to decrease as heart rate increases, with the deviation signals of subjects with low heart rates being very similar. In addition, the IVS tends to be more similar to the deviation signal representing aggregate vessel motion than the deviation signals representing each individual vessel. This suggests that the IVS is a better predictor for aggregate vessel motion than for specific vessel motion. The deviation signal of the IVS is least similar to that of the RCA.

D. Comparison of Optimal Quiescent Phases to those Predicted by the CT Scanner

The optimal quiescent phase of the coronary vessels when taken in aggregate was compared to the nearest systolic or diastolic quiescent phase predicted from the ECG by the CT scanner for each subject. The results of this comparison are shown in Fig. 6. The average absolute difference in terms of phase is 5.1% suggesting that the ECG-based method used for predicting quiescence is not optimal. Fig. 6 also shows that there is no bias toward under- or over-prediction and that the predicted

TABLE III. Average Correlations of Deviation Signals

Low Heart Rate						
	LM	LAD	LCX	RCA	AGG	IVS
LM	1.00	0.92	0.89	0.82	0.91	0.87
LAD	—	1.00	0.85	0.79	0.85	0.83
LCX	—	—	1.00	0.76	0.91	0.82
RCA	—	—	—	1.00	0.86	0.82
AGG	—	—	—	—	1.00	0.84
IVS	—	—	—	—	—	1.00

Medium Heart Rate						
Med. HR	LM	LAD	LCX	RCA	AGG	IVS
LM	1.00	0.83	0.91	0.76	0.90	0.77
LAD	—	1.00	0.87	0.61	0.84	0.78
LCX	—	—	1.00	0.73	0.92	0.76
RCA	—	—	—	1.00	0.85	0.67
AGG	—	—	—	—	1.00	0.81
IVS	—	—	—	—	—	1.00

High Heart Rate						
High HR	LM	LAD	LCX	RCA	AGG	IVS
LM	1.00	0.65	0.75	0.68	0.86	0.63
LAD	—	1.00	0.72	0.51	0.67	0.53
LCX	—	—	1.00	0.59	0.79	0.78
RCA	—	—	—	1.00	0.86	0.57
AGG	—	—	—	—	1.00	0.64
IVS	—	—	—	—	—	1.00

Dashes represent symmetric entries about the diagonal.

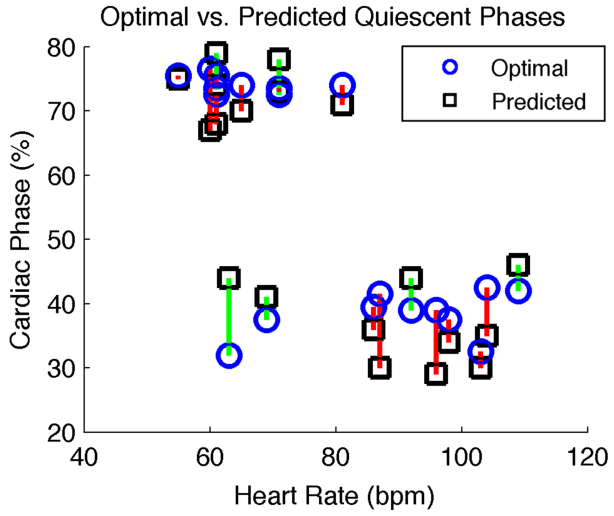

FIG. 6. Comparison of the phase predicted by the CT machine to the calculated optimal quiescent phases of the aggregate vessel motion for each subject. Optimal and predicted phases are indicated by blue circles and black squares, respectively. The line connecting the optimal and predicted phases is red if the predicted phase occurs before the optimal phase and green otherwise.

phases are more variable than the actual optimal phases.

IV. DISCUSSION

To better understand cardiac quiescence, two novel robust methods for quantifying the cardiac quiescence of specific cardiac features from cardiac CT reconstructions were developed. These methods are based on a deviation measure calculated from the phase-to-phase correlation of each cardiac feature. Understanding cardiac quiescence is critical to the performance of many cardiac imaging modalities, including CTCA, that rely on acquiring imaging data while the heart is relatively stationary.

To analyze the quiescence of the LM, LAD, LCX, RCA, and IVS, a novel semi-automated method was developed to segment each cardiac feature. An undersampled number of axial slices were manually segmented. The segmentations for the missing slices were then interpolated from the neighboring manually-segmented slices. When compared to manually segmenting each slice, this approach resulted in an average speed-up by a factor of 3 for the coronary vessels and 8 for the IVS. A manually-guided, semi-automated approach to segmentation was needed because reconstructions containing motion artifacts would prove problematic for a completely automated approach.

The coronary vessels and the IVS were investigated for 20 patients. The systolic and diastolic quiescent periods were found to be similar across cardiac features. The statistics of the quiescent periods showed a dependency on subject heart rate. This was most notable for the duration of the diastolic quiescent period, which was much shorter for high heart rates (above 85 bpm). As can be seen from Table I, the longest quiescent phase transitions from diastole to systole as heart rate increases. This is in line with the accepted consensus that the optimal gating window occurs in diastole for low heart rates and systole for high heart rates [8, 9].

The optimal quiescent phase of each coronary vessel, the vessels taken in aggregate, and the IVS were detected by finding the most quiescent period with a length of 83 ms. This duration corresponds to the minimum acquisition time of the CT scanner used for this work. The optimal quiescent phase of the RCA was found to transition from diastole to systole at a lower heart rate than the other coronary vessels. On the other hand, the optimal quiescent phase of the IVS was found to transition at a higher heart rate than the coronary vessels.

For each subject, the coronary vessels, the vessels taken in aggregate, and the IVS were compared to observe the overall motion similarity among the different cardiac features. The similarity between the features was high for

low heart rates and decreased as heart rate increased. The motion of the IVS was found to be more similar to the aggregate vessel motion than the motion of individual vessels, suggesting that the IVS is a better predictor of aggregate vessel motion than for specific vessel motion.

To assess the accuracy of the quiescent phases predicted by the CT scanner, the optimal quiescent phase of the coronary vessels taken in aggregate were compared against the predicted best phase by the CT scanner for each subject. The predicted phases were found to differ from the optimal phases by an average of 5.1% in terms of absolute phase difference. Also, the difference between the optimal and predicted quiescent phases showed no positive or negative bias and did not trend with heart rate. Taken together, this suggests that there is room for improvement in predicting cardiac quiescence for the purpose of gating cardiac CT acquisition.

The IVS was found to be a suitable predictor of vessel quiescence, especially for aggregate vessel quiescence. Aggregate vessel quiescence is most important in terms of cardiac imaging, as it is typically desired to diagnose all coronary vessels from one exam. Liu *et al.* showed that the IVS was an accurate predictor of LAD vessel quiescence [10]. From Table III, the LAD is in fact among the least similar to the IVS, suggesting that if the IVS is a suitable predictor for the LAD it will be as good or better for the other vessels. The quiescence of the IVS is of particular interest because it can be readily observed using echocardiography, as opposed to the coronary vessels. The use of echocardiography to analyze cardiac quiescence is extremely useful because it is a real-time visualization of cardiac state. By verifying the relationship between the IVS and the coronary vessels, echocardiography can be used to analyze cardiac quiescence on a beat-by-beat basis [6].

A. Limitations

A limitation of this work is that the diagnostic quality of the CTCA images is not observed directly. Though it seems logical that data acquired during more quiescent phases of the cardiac cycle will produce coronary images of better diagnostic quality, it is necessary as a next step to determine the potential improvement in diagnostic quality that could be attributed to more accurate gating. This improvement is most likely a function of heart rate and quiescent period duration. The diagnostic quality of the coronary vessels as a function of heart rate is addressed in [11], where radiologists graded the diagnostic quality at 10% intervals of the cardiac cycles for a large number of patients separated into low, medium, and high heart rate ranges. Addressing the diagnostic quality as a function of heart rate at a finer interval and on a patient-by-patient basis is a topic of current research.

Another limitation is that the CT reconstructions used in this work only covered the range of 20%–80% of the cardiac cycle. This range of the cardiac cycle was chosen because it has been shown to contain the optimal systolic and diastolic quiescent phases [3, 12]. However, since every phase of the cardiac cycle is not reconstructed, it is possible that the start of the systolic or end of the diastolic quiescent period may lie outside the 20%–80% reconstructed interval of the cardiac cycle. This is apparent in Fig. 5, where a number of quiescent periods begin either at 20% or end at 80%. This may explain the difference between the phase of the quiescent period centers and the optimal quiescent phases. An artificially truncated quiescent period will be biased away from the boundaries of the reconstructed interval. This is because each quiescent period center is defined as the midpoint between the beginning and end of that quiescent period. On the other hand, the method used to find the optimal quiescent phase is independent of the beginning and end phase of the quiescent period.

Lastly, by observing motion directly from CT reconstructions, beat-to-beat heart rate variability is not taken into account. This is because the CT reconstructions are created from data acquired over multiple cardiac cycles. Observing intra-subject variability is important to understand how it affects diagnostic quality. It has been shown that as heart rate variability increases the diagnostic image quality decreases [13]. For this reason, it is also important to observe quiescence on a beat-by-beat basis, suggesting that echocardiography and other signals derived directly from cardiac motion will be complementary in the analysis and prediction of cardiac quiescence.

B. Conclusion

A robust approach for identifying and analyzing cardiac quiescence was developed. The center and duration of the quiescent periods were found and the optimal quiescent phases were computed for each subject. The predicted best reconstruction phases by the CT scanner from the ECG were found to differ from the optimal quiescent phases by 5% in terms of absolute phase. The method used to compute the optimal phase could potentially be used by the CT scanner to accurately determine the best phase to reconstruct for retrospective cardiac exams. Lastly, the IVS was found to be a suitable predictor of vessel quiescence, suggesting the applicability of echocardiography as a tool for observing quiescence on a beat-by-beat basis.

ACKNOWLEDGMENT

The authors would like to thank William Landreth, RT and Lucienne McKinney, RT of the Department of Radiology and Imaging Sciences, Emory University Hospital for their time and assistance with obtaining the necessary data to complete this study.

[1] B. Desjardins and E. A. Kazerooni, AJR Am J Roentgenol **182**, 993 (2004).

[2] S. Tridandapani, J. B. Fowlkes, and J. M. Rubin, Journal of Ultrasound in Medicine **24**, 1519 (2005).

[3] K. R. Johnson, S. J. Patel, A. Whigham, A. Hakim, R. I. Pettigrew, and J. N. Oshinski, J Cardiovasc Magn Reson **6**, 663 (2004).

[4] V. L. Roger, A. S. Go, D. M. Lloyd-Jones, E. J. Benjamin, J. D. Berry, W. B. Borden, D. M. Bravata, S. Dai, E. S. Ford, C. S. Fox, H. J. Fullerton, C. Gillespie, S. M. Hailpern, J. A. Heit, V. J. Howard, B. M. Kissela, S. J. Kittner, D. T. Lackland, J. H. Lichtman, L. D. Lisabeth, D. M. Makuc, G. M. Marcus, A. Marelli, D. B. Matchar, C. S. Moy, D. Mozaffarian, M. E. Mussolino, G. Nichol, N. P. Paynter, E. Z. Soliman, P. D. Sorlie, N. Sotoodehnia, T. N. Turan, S. S. Virani, N. D. Wong, D. Woo, M. B. Turner, and American Heart Association Statistics Committee and Stroke Statistics Subcommittee, Circulation **125**, e2 (2012).

[5] M. R. Patel, E. D. Peterson, D. Dai, J. M. Brennan, R. F. Redberg, H. V. Anderson, R. G. Brindis, and P. S. Douglas, N. Engl. J. Med. **362**, 886 (2010).

[6] C. A. Wick, J. H. McClellan, L. Ravichandran, and S. Tridandapani, Translational Engineering in Health and Medicine, IEEE Journal of , 1 (2013).

[7] M. Svedlow, C. D. McGillem, and P. E. Anuta, IEEE Transactions on Aerospace and Electronic Systems , 141 (1978).

[8] S. Leschka, S. Wildermuth, T. Boehm, L. Desbiolles, L. Husmann, A. Plass, P. Koepfli, T. Schepis, B. Marincek, P. A. Kaufmann, and H. Alkadhi, Radiology **241**, 378 (2006).

[9] A. C. Weustink, N. R. Mollet, F. Pugliese, W. B. Meijboom, K. Nieman, M. H. Heijenbrok-Kal, T. G. Flohr, L. A. E. Neefjes, F. Cademartiri, P. J. de Feyter, and G. P. Krestin, Radiology **248**, 792 (2008).

[10] G. Liu, X.-L. Qi, N. Robert, A. J. Dick, and G. A. Wright, Med Phys **39**, 3009 (2012).

[11] M. B. Srichai, E. M. Hecht, D. Kim, J. Babb, J. Bod, and J. E. Jacobs, J Cardiovasc Comput Tomogr **3**, 300 (2009).

[12] H. Seifarth, S. Wienbeck, M. Püsken, K.-U. Juergens, D. Maintz, C. Vahlhaus, W. Heindel, and R. Fischbach, AJR Am J Roentgenol **189**, 1317 (2007).

[13] H. Brodoefel, C. Burgstahler, I. Tsiflikas, A. Reimann, S. Schroeder, C. D. Claussen, M. Heuschmid, and A. F. Kopp, Radiology **247**, 346 (2008).